Journal of Materials Chemistry C

Accepted Manuscript

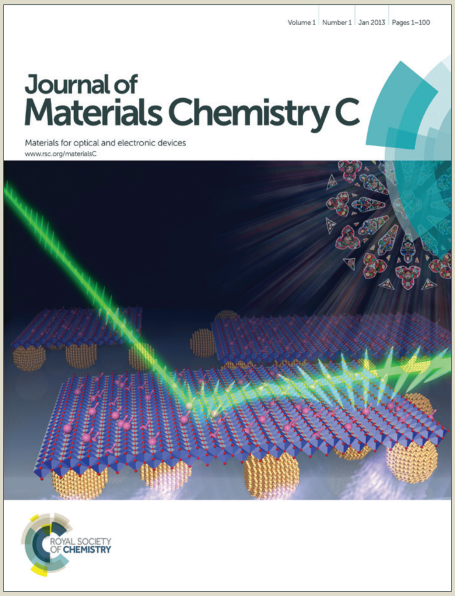

ROYAL SOCIETY OF CHEMISTRY

www.rsc.org/materialsC

Tunable Electronic Structure and Mechanical Properties of Halogenated Silicene: A First-Principles Study

Wei-Bing Zhang,[*a] **Zhi-Bo Song,**[a] **and Liu-Ming Dou**[a]

Received Xth XXXXXXXXXX 20XX, Accepted Xth XXXXXXXXX 20XX
First published on the web Xth XXXXXXXXXX 20XX
DOI: XX.XXXX/b000000x

We have investigated the geometry, electronic structure and mechanical properties of halogenated silicene XSi (X=F,Cl,Br and I) in various conformers from first principles systemically. The energetics, structure, band structure, elastic constants and the corresponding modulus are given in detail. Our results indicate that halogenated silicene shows an enhanced stability compared with silicene and present the moderate and tunable direct gap with small carrier effective mass. The element- and conformer-dependence of energy gap can be understood well by the variance of buckling and a bond energy perturbation theory based on orbital hybridization. Moreover, the direction-dependent mechanical properties are also calculated and discussed. Interestingly, a negative Poisson ratio is predicted in fluorinated silicene with boat2 structure. The enhanced stability, moderate energy gap,small carrier effective masses and improved mechanical properties predicted here promise halogenated silicene as the promising candidate in future electronic device.

1 Introduction

Silicene, a two-dimensional buckled honeycomb arrangement of silicon atoms, has received tremendous attention recently both experimentally and theoretically.[1–6] Similar to graphene, silicene has the promising linear dispersion (Dirac cone) at the *K* points of the Brillouin zone. Moreover, because of the compatibility with the matured silicon-based electronics and the existing semiconductor fabrication processes, silicene is excepted to be more exciting than graphene. In addition, the silicene is also proposed as a candidate of topological insulator since its strong spin-orbit coupling.[7,8]Although silicene is considered as a promising candidate for further electronics, its lack of a band gap leads to a small current on/off ratio in field-effect transistors (FETs) similar to graphene. The pristine silicene thus is unsuitable for digital electronic applications, in which an excellent switching capability is needed. Meanwhile, silicene must be grown on metallic substrates and cannot be exfoliated from substrates. Thus, it is increasingly interesting to discover silicene derivative with exceptional stability and optoelectronic properties.

Significant effort has been devoted to open a band gap and several routes such as quantum confinement[9] and strain[10] have been proposed in such a Dirac system. Chemical functionalization is another effective method to band gap engineering of two-dimensional material.[11,12] For example, hydrogenation and fluorination are found to be able to tailor the electronic properties of graphene effectively and lead to the outstanding electronic properties.[11,12] Recently, a graphane (CH) analogue germanane (GeH)[13] with resistance to oxidation and good thermal stability has been synthesized recently. A direct band gap of 1.53 eV and an electron mobility about five times higher than that of bulk Ge are predicted theoretically. Germanane is thus proposed as a promising candidate for a wide range of optoelectronic and sensing applications.

Intriguing by the rich physical properties found in graphane analogue shown above, chemical functionalization has also been suggested in the case of silicene. Earlier study[14–17] suggests that hydrogenation and fluorination can open band gaps in the silicene sheet. Gao *at al.*[17] have investigated the electronic structures of halogenated silicene including F, Cl, Br and I using the density functional theory based screened exchange local density approximation method (sX-LDA). They suggested that the energy gap of X-silicene firstly increases and then decreases with number of periodic number. Pioneer investigations of graphane[18] have proposed four possible low-energy conformers namely chair, boat,chair2 and boat2 for graphane (CH) and the analogues.However, most of the calculations are still only limited to the simple chair conformer. Recently, Ding *et al.*[19] have systematically investigated the structures and properties of fluorinated and hydrogenated silicene using first-principles calculations, in which four possible conformers are considered. The results indicate that the fluorination prefers the conformation with a zigzag-line buckling (*i.e.* chair2 using notation given in Ref.[18]), which suggests that more conformers should be considered to reach the con-

---

[a] *School of Physics and Electronic Sciences, Changsha University of Science and Technology, Changsha 410004, People's Republic of China. Fax: +86(0)73185258217; Tel: +86(0)73185258223; E-mail: zhangwb@csust.edu.cn ; weibingzhangavh@gmail.com*

vincing conclusion.

On the other hand, the 2D crystals have been suggested as the key components in future flexible electronics devices, due to the possible outstanding electronic properties, and atomic thickness. A detailed knowledge of their mechanical properties is a necessary prerequisite to any practical device applications. Despite the tremendous scientific and technological interest, a detailed knowledge of mechanical properties of halogenated silicene still lack completely. Besides the electronic structure which has been focused already, it is thus quite interesting to investigate the various properties including the elastic properties of halogenated silicene theoretically.

In the present work, we have investigated the halogenated silicene XSi (X=F, Cl, Br, and I) systemically, in which four possible conformers are considered. The geometry, electronic structure, carrier effective mass and elastic properties are given in detail . And the underlying mechanism are analyzed.

2 COMPUTATIONAL DETAILS

The present calculations have been performed using QUANTUM ESPRESSO package, which is an integrated suite of computer codes for electronic-structure calculations and materials modeling, based on density-functional theory, plane waves, and pseudopotentials[20]. General gradient approximations(GGA) in the Perdew-Burke-Ernzerhof (PBE) implementation[21] were chosen for the exchange correlation functional and the ultrasoft pseudopotentials were used. Convergence tests have been performed carefully both for plane-wave cutoff energy and *k* point sampling. A plane-wave basis set with a kinetic energy cutoff of 50 Ry for wave functions and 500 Ry for charge densities were used. The Brillouin zone sampling with a mesh of $16 \times 16 \times 1$ generated by the scheme of Monkhorst-Pack[22] was chosen for FSi with chair conformer, and the same *k* density is used to sample the Brillouin zone of other systems. All the lattice constants and atom coordinates are optimized using BFGS quasi-newton algorithm until the maximum force on all atoms is less than 10^{-4} *Ry/Bohr*. A large vacuum space at least 18 Å is used in supercell to avoid interactions between images. The elastic constants are obtained by energy-strain approach, in which deformations applied in unit cell and the corresponding energy-strain relationship can be found in Ref.[23]. The direction dependent Young modulus and Poisson ratio are also obtained following the same procedure present there. Phonon dispersion curves have been obtained by means of density-functional perturbation theory,[24] in which the dynamical matrices are calculated on a $5 \times 5 \times 1$ mesh for halogenated silicene in chair conformer.

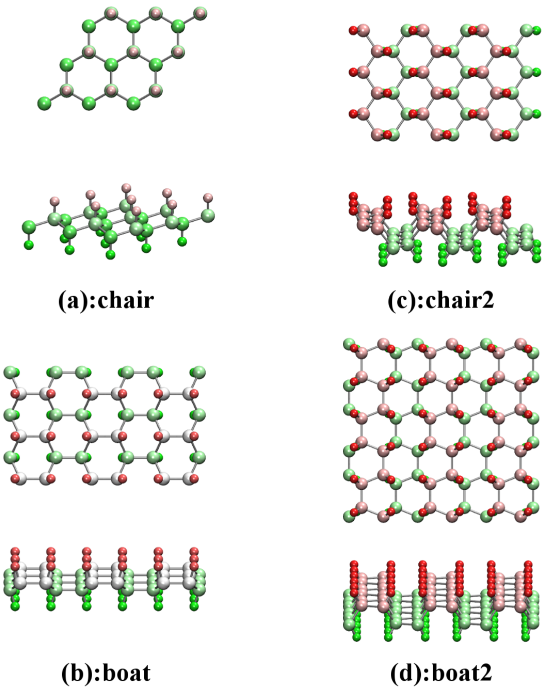
(a):chair **(c):chair2**

(b):boat **(d):boat2**

Fig. 1 (Color online) Structural models of different conformers of halogenated silicene. (a)-(d) represent the chair, boat , chair2 and boat2 conformers, respectively. The Si and halogenated atoms are represented by small and big balls in the figure, while the heights of different atoms are represented by colors ranging from green (low) to red (high).

3 Results and Discussion

3.1 Energetics and Geometry

Firstly, we give the energetics of halogenated silicene with various conformers. To evaluate the stability of X-silicene, the formation energy are calculated and given in Tab. 1. The formation energy per SiX unit is defined by $E_f = \frac{1}{n_{Si}}(E_{total} - \frac{n_{Si}}{2}E_{Silicene} - \frac{n_X}{2}E_{X2})$, whereas E_{total}, $E_{Silicene}$ and E_{X2} are the total energies of halogenated silicene, silicene and singlet halogen molecule. The negative E_f indicates that halogenation of silicene is an exothermic reaction and the corresponding halogenated-silicene should be stable. Our calculation indicate that E_f of all halogenated silicene considered here are negative, which suggests a higher stability of halogenated-silicene with respect to silicene. Although silicene has already been grown epitaxially and investigated on different metallic substrates in high vacuum,[3,4] there are still some lively debates about the stability of silicene isolation from its parent substrate or exposure to air.[25,26]The enhanced stability of halogenated silicene can open a new routine to synthesize stable silicene derivative experimentally. Interestingly,

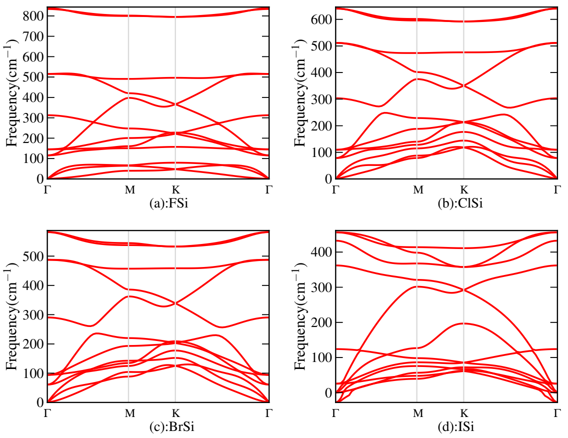

Fig. 2 (Color online) Phonon dispersion relations of halogenated silicene in chair conformer.

a graphane (CH) analogue germanane (GeH)[13] has been synthesized recently, which can be stable in air over 5 months and also shows high carrier mobilities. We also found that the most stable conformer of FSi is chair2, following by chair, boat2 and boat, which is also in good agreement with earlier study.[19] Where for the other XSi(X=Cl,Br,I),the energy order changes to chair $<$ chair2 $<$ boat $<$ boat2, and the lowest energy structure is chair conformer. To clearly show the element and conformer dependence of formation energy of halogenated silicene, we also present the formation energy result in Fig. 3-(a). As shown in figure, we can also find that the formation energy shows very weak conformer dependence while the absolute value of formation energy decreases monotonically with periodic number. This suggests that the stability decreases monotonically with periodic number and four conformers should be considered due to the similar formation energy. The weakening stability in iodide is also found in halogenated graphene.[27] Graphene iodide are found to be unstable after relaxation. Phonon dispersion is used to confirm the stability of materials. As an illustrated example, we have investigated the phonon dispersion of XSi (X=F, Cl, Br, and I) in chair conformer to evaluate the stability of halogenated silicene. As shown in Fig. 2, the imaginary frequency is found to be absent in halogenated silicene except the case of ISi, whereas small negative frequencies appear near Gamma points. This suggests the halogenated silicene XSi (X=F, Cl, Br) is stable whereas the stability of ISi seems to be weakening, which is in good agreement with the trend of formation energy. In addition, the phonon frequency of halogenated silicene is found to be softening monotonically from F to I due to the increasing atomic weight.

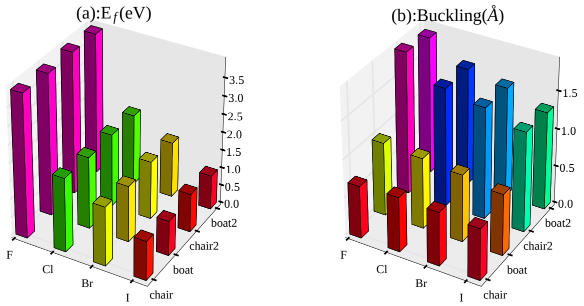

Fig. 3 (Color online) The absolute value of formation energy and buckling of halogenated silicene in different conformers.

Now turn our attention to the change of geometry after halogenation of silicene. We can find clearly in Table. 1 that the lattice parameters are found to increase in halogenated silicene. Due to the mixture of sp^2 and sp^3 orbital hybridization , the silicon atoms in silicene present a low buckling, which is also the main difference of silicene from graphene. The buckling of silicon layer in silicene is found to increase after halogenation, which can be understood by the fact that hybridization in halogenated silicene is more closed to sp^3 hybridization. As shown in Fig. 3-(b), for halogenated silicene in the same conformer, buckling decreases with element number except chair. Whereas for compounds with the same element, the buckling seems to increase from chair, boat ,chair2 to boat2. In addition, we can also find that the distance between Si and Si atoms shows a non-monotonic variance whereas the distances between Si and halogen element increase linearly with periodic number. This is also in line with the change of distance of CX species with periodic number in halogenated graphene.[27] The change of geometry is related to gap opening in halogenated silicene, which will be discussed in detail below.

3.2 Energy band

As shown above, the lack of gap in pristine silicene limits its application in practical electronic device. Opening a gap in silicene has attracted a lot of attention recently. The energy gaps of halogenated silicene calculated using PBE functional are listed in Tab. 1. We can find that a tunable energy gap ranging from 0.54 eV to 2.08 eV opens in halogenated silicene. Moreover, most of compounds have a direct gap except ISi with boat, chair2 and boat2 structure. Using the same PBE calculation, energy gaps above 3.20 eV were found in graphene fluoride CF with various conformers in previous study.[27,28] It's well known that silicon, the wildly-used electronic material, has a indirect gap of 1.13 eV. Due to the comparable energy gap and compatibility with silicon, the halogenated silicene is

Table 1 The calculated energetics, geometry and band gap of halogenated silicene.

	FSi				ClSi				silicene
	chair	boat	chair2	boat2	chair	boat	chair2	boat2	
a_{zig} (Å)	3.969	3.962	3.944	6.617	3.946	3.915	3.958	6.871	3.867
a_{arm}(Å)		6.670	5.640	6.933		6.866	6.283	7.365	
Z_b(Å)	0.692	0.970	1.890	1.827	0.722	0.935	1.572	1.560	0.452
d^{inter}_{Si-Si}(Å)	2.394	2.411	2.398	2.393	2.390	2.386	2.378	2.381	2.278
d_{Si-X}(Å)	1.639	1.640	1.636	1.637	2.079	2.078	2.080	2.078	
E_f(eV)	-3.961	-3.930	-3.965	-3.936	-2.040	-1.988	-2.015	-1.974	
gap(eV)	0.718	0.618	0.835	0.904	1.280	1.186	1.643	1.897	

	BrSi				ISi			
	chair	boat	chair2	boat2	chair	boat	chair2	boat2
a_{zig}(Å)	3.976	3.937	4.002	7.059	4.062	4.002	4.105	7.397
a_{arm}(Å)		7.051	6.464	7.510		7.386	6.750	7.783
Z_b(Å)	0.708	0.890	1.477	1.463	0.680	0.811	1.322	1.297
d^{inter}_{Si-Si}(Å)	2.402	2.399	2.385	2.388	2.442	2.432	2.403	2.409
d_{Si-X} (Å)	2.250	2.249	2.251	2.248	2.480	2.480	2.482	2.479
E_f (eV)	-1.631	-1.552	-1.603	-1.535	-1.082	-0.962	-1.060	-0.946
gap(eV)	1.235	1.176	1.677	2.083	0.543	*0.6328*	*1.240*	*1.058*

expected to server as a possible candidate of future electronic and optoelectronic device. In addition, carrier effective mass is another important physical quantity in electronic material. Since the effective mass is direction-dependent in k space, we calculate carrier effective masses of valence band maximum (VBM) and conduction band minimum (CBM) along two different direction. As shown in Tab. 2, m^*_l (m^*_r)represents the effective masses from the left (right) of VBM(CBM), which corresponds the K-Γ (M-Γ) in chair conformer and Y-Γ (X-Γ) in the other ones. During the calculation, 60 points are sampling along the high-symmetry lines (e.g. K-Γ) and 10 points near Γ are used in the fitting procedure. We can find the effective masses is highly anisotropic in halogenated silicene and some of effective masses are comparable with silicon, which thus implies a high mobility in such system. However, it should be noticed that the gap present here are based on the semi-local PBE functional, which is known to underestimate the gap of material. Further work using high-level theory to obtain reliable energy gap and optical properties are in progress.

For further insight into the gap formation mechanism , the element-projected densities of state of halogenated silicene with different conformers are given in Fig. 4. We can find clearly that the orbital hybridization shows a very weak conformer dependence but very sensitive to halogen element. Meanwhile, this element dependence seems to be more noticeable in VBM while the hybridization seems to be invariance in CBM except boat2 conformer. As shown in figure, we can find that orbital contributions of halogen element are less than 20% at CBM and seem to remain the same for all structures

Table 2 The calculated carrier effective masses given in unit of the free electron mass (m_e) of halogenated silicene .

		hole		electron	
		m^*_l/m_e	m^*_r/m_e	m^*_l/m_e	m^*_r/m_e
FSi	chair	0.669	0.687	0.239	0.220
	boat	0.154	0.671	0.306	0.988
	chair2	0.152	1.142	0.960	0.796
	boat2	0.578	0.414	0.763	0.644
ClSi	chair	0.789	0.813	0.219	0.209
	boat	0.175	0.886	0.189	0.933
	chair2	0.184	1.512	0.936	1.411
	boat2	0.885	0.570	0.885	0.733
BrSi	chair	0.959	0.993	0.194	0.184
	boat	0.189	1.121	0.173	0.989
	chair2	0.216	4.999	0.135	2.857
	boat2	0.986	2.964	0.706	0.197
ISi	chair	1.324	1.378	0.128	0.120
	boat	0.207	1.702	0.511	0.178
	chair2	1.146	1.223	0.149	2.293
	boat2	0.239	2.759	0.627	0.176

except the boat2 conformers, in which the orbital contribution increases from 20% in FSi to about 40% in XSi(X=Cl,Br and I). At VBM, orbital contribution of halogen element seems to increase with periodic number from FSi(less than 20%), ClSi(about 20%), BrSi(about 40%) to ISi(about 80%).

As shown in Tab. 1 and Fig. 5-(c), we can find that with the same element, the energy gap increases from chair , boat , chair2 to boat2, which is in line with the change of buckling in halogenated silicene present in Fig. 3-(b). Leenaerts *et al.*[28] have investigated graphene fluoride in various configurations and found that the energy gap increases from chair, boat, chair2 (Zigzag labeled in Ref.[28]) to boat2 (Armchair). This trend is consistent with present results for halogenated silicene. It is well accepted that the buckling of silicene can be seen as consequence induced by the mixture of sp^2 and sp^3 orbital of silicon atoms. In the case of halogenated silicene, the binding is more close to sp^3 hybridization in diamond silicon. Large buckling of silicon will lead to gap opening in silicene. Since the orbital contribution in halogenated silicene is conformers insensitive, the variance of buckling with conformers are responsible for the change of band gap in halogenated silicene.

On the other hand, the change of energy gap with element seems to be more complicated. As shown in Fig. 5-(c), the energy gap increases from F to Cl then decreases from Cl to I in the case of chair, boat, and chair2. For boat2 conformer, the gap of BrSi is found to be larger than ClSi, which is different from the other conformers. Band gaps of graphene halides in chair configuration have also been studied carefully by Karlický*et al.*,[27] in which the energy gap is found to increase with periodic number. Following the previous work about halogenated silicene in chair conformer by Gao *et al.*[17], element dependence can be understood well by bond energy perturbation suggested by Sun[29]. The change of bond energy will induce a perturbation of the Hamiltonian, and thus Eg. Specifically, the increase (reduction) of bond energy will lead to increase (decrease) of E_g.

Halogens functionalization in silicene modulates the bond length and bond energy of Si-Si and Si-X. As seen in Fig. 5, with increasing of periodic number, we can find the distances of Si-X bond increase linearly whereas the Si-Si bond decreases from F to Br but increases hereafter in all conformers considered here. Previous projected energy band (Fig. 4) analysis has suggested that orbital contributions of Si atoms are larger than halogen element in the case of FSi and ClSi, thus the Si-Si bond dominated the system. The decreasing bond distance of Si-Si will lead to the increase of Si-Si bond energy, thus increase the energy gap. For BrSi, the Br and Si atoms contribution equivalent in the VBM, thus the bond energy of Si-Si and Si-X will contribute to energy gap equivalently. d_{Si-Si} and d_{Si-X} increase from Cl to Br, which leads E_{Si-Si} and E_{Si-X} decrease, thus the corresponding energy gap decreases. For ISi compounds, Si-X dominated the system due to large contribution of I element at VBM, whereas E_{Si-X} decrease and gap decrease. Such a gap formation mechanism can be well applied in chair, boat and chair2 conformers but fails in the case of boat2 structure.

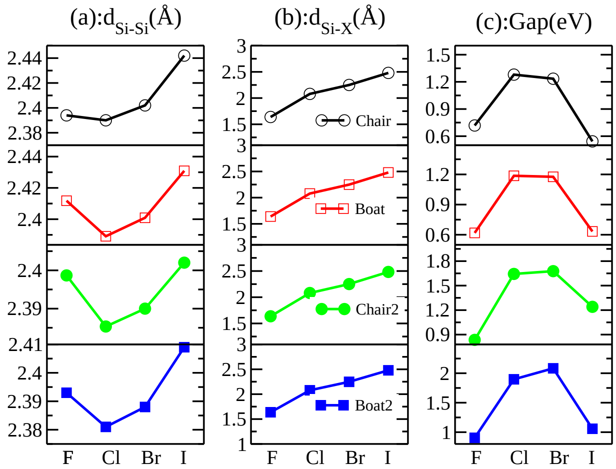

Fig. 5 (Color online) The energy gap, d_{Si-Si}, and d_{Si-X} of halogenated silicene in different conformers.

The success and failure of such a mechanism can be ascribed to the variance of CBM with element number for different conformers. To understand the gap formation mechanism in all conformers, bond energy perturbation suggested before should be extended. The completion between movement of CBM and VBM should be responsible to gap formation of halogenated silicene. In the case of chair, boat and chair2 conformers, since the hybridization at CBM with is almost insensitive to element , the decreasing of gap from Cl to Br can be understood as following: i) decreasing bond energy will make VBM move towards high-energy region relative to Fermi level.ii) the CBM are not affect due to the invariance of hybridization at CBM . For boat2, the contribution of halogen element increases from F to I for boat2 at CBM, the CBM will also move towards high-energy region as VBM. From the Cl to Br element, the magnitude of movement of CBM seems to be larger than VBM, which thus leads to a increasing gap in boat2 conformer.

3.3 Elastic properties

To realize a material for new-generation device applications such as flexible electronics, a complete knowledge of their mechanical properties is required. The elastic constants of all halogenated silicene conformers as well as pristine silicene calculated using the method developed for graphene[23] are reported in Table. 3. The calculated in-plane Youngs modulus E and Poisons ratio v of silicene is 61.87 Nm^{-1} and 0.29, which

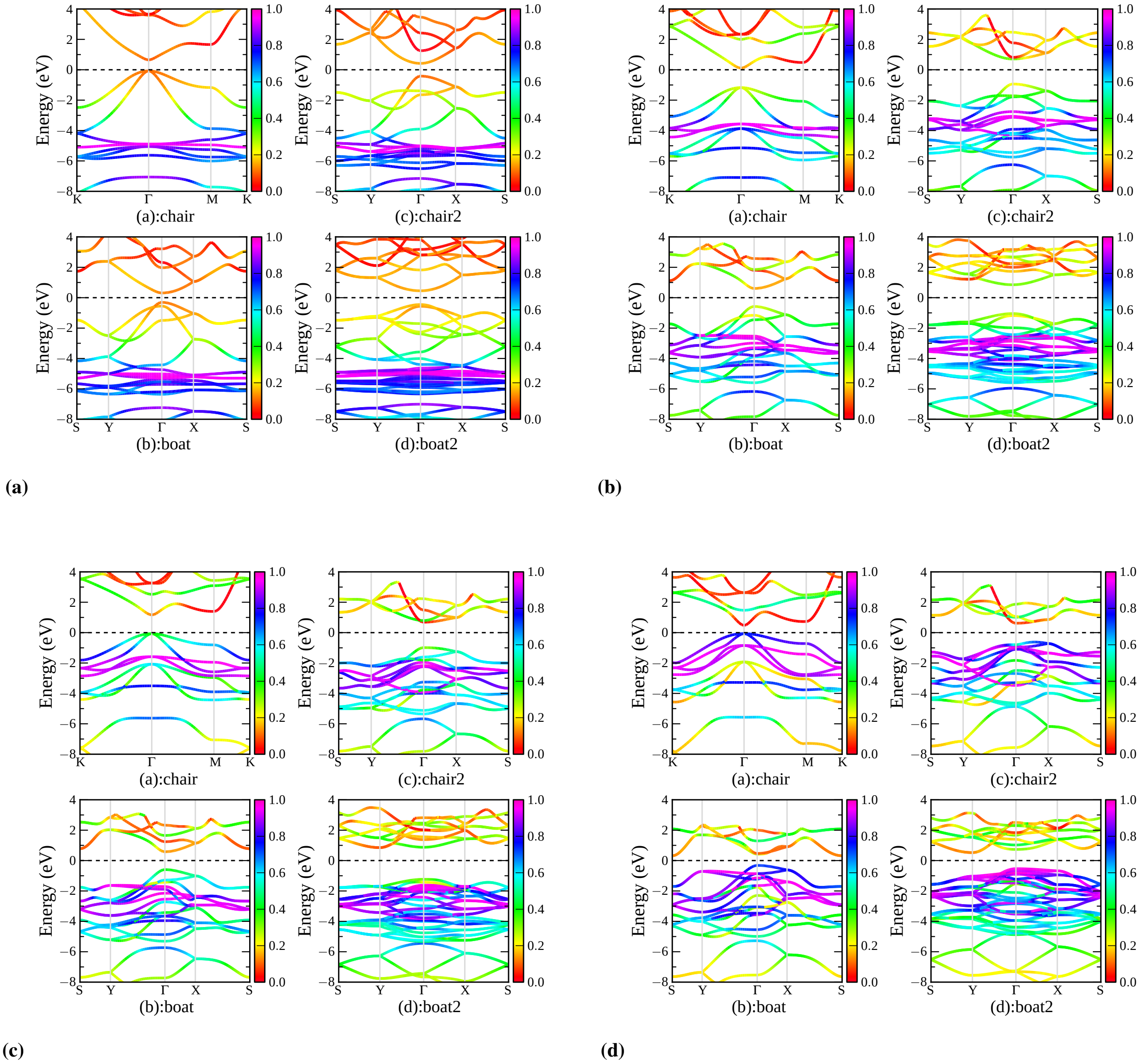

Fig. 4 (Color online)Electronic band structure of halogenated silicene in four different conformers. The contributions from halogenated element to the bands are represented by colors. (a)-(d) represent the FSi, ClSi , BrSi and ISi compounds, respectively.

Table 3 The calculated elastic properties (in units of Nm^{-1}) of halogenated silicene.

	conformers	c_{11}	c_{22}	c_{44}	c_{12}	E_{min}	E_{max}	υ_{min}	υ_{max}
Silicene		67.71	67.71	23.91	19.89	61.87	61.87	0.29	0.29
FSi	chair	50.86	50.86	19.77	11.32	48.34	48.34	0.22	0.22
	boat	39.06	51.56	4.65	3.83	15.59	51.15	0.07	0.68
	chair2	18.46	64.56	15.28	5.99	17.9	62.62	0.03	0.32
	boat2	21.56	45.27	15.49	-0.99	21.54	45.22	-0.05	-0.02
ClSi	chair	56.67	56.67	21.68	13.31	53.54	53.54	0.23	0.23
	boat	66.59	57.58	16.54	6.81	44.51	65.78	0.1	0.35
	chair2	40.53	60.63	18.6	10.42	38.74	57.95	0.17	0.26
	boat2	45.48	69.03	15.31	4.55	39.47	68.57	0.07	0.32
BrSi	chair	59.23	59.23	22.11	15.01	55.42	55.42	0.25	0.25
	boat	73.53	60.79	14.65	6.01	41.63	72.93	0.08	0.43
	chair2	49.45	62.02	20.83	12.68	46.85	58.77	0.2	0.26
	boat2	55.44	75.57	13.94	4.34	39.35	75.22	0.06	0.42
ISi	chair	63.72	63.72	24.3	15.13	60.13	60.13	0.24	0.24
	boat	78.91	66.87	8.19	3.51	26.94	78.72	0.04	0.65
	chair2	58.43	61.5	23.01	15.42	54.56	57.6	0.24	0.26
	boat2	64.66	79.99	9.58	2.63	30.43	79.85	0.03	0.59

are in good agreement with earlier calculations.[30,31] This indicates that the present calculation should be reliable. Compared with pristine silicene, the elastic constants of halogenated silicene in the chair and chair2 conformer decrease after halogen element functionalization, while boat and boat2 structures tend to have higher elastic constants. On the other hand, we also find clearly that with the same conformer, the elastic constants increase monotonically from F to I. This agrees with the change of orbital hybridization shown in Fig. 4. It is can be excepted that the materials with stronger Si-X hybridization should reduce the strain to smaller when loading the same stress, which thus leads to larger elastic constants.

Moreover, we also explored anisotropic linear elastic behavior of halogenated silicene. The $\vec{n}$ dependence of E and ν for the halogenated silicene are given in Fig. 6 and Fig. 7. A perfect circular shape of the $E_{\vec{n}}$ and $\nu_{\vec{n}}$ plots can be found in the case of silicene and halogenated silicene with chair conformer, which indicates a fully isotropic elastic behavior. Boat and boat2 structures are found to be much more anisotropic than the chair2 structure. We can also find that both Young modulus E and Poisson ratio ν of halogenated silicene with chair and chair2 conformers is smaller than pristine silicene whereas boat and boat2 structures show much improved elastic modulus in certain direction. The extremes of Young modulus E curve are found to locate along armchair and zigzag direction whereas for the ν, extremes direction is around 45° . In addition, with increasing of element numbers, the elastic modulus are found to be more close to the circle of the silicene , which indicates that the value increases monotonically from F to I.

Most interestingly, a intriguing unconventional negative Poissons ratio ranging from -0.05 to -0.02 are found to in a F-silicene with boat2 conformer. The negative Poisson ratio can be found in all direction and the value is comparable with that found recently in single-layer black phosphorus.[32] Since the crystal structure of boat2 conformers resembles the black phosphorus, the mechanism of negative Poisson ratio should be similar with each other. It should be noticed that there is still a debate about the negative Poisson ratio found in single-layer black phosphorus. Using the vasp code with plane-wave basis sets, Ding *et al.*[33] found the minimum Poisson ratio of phosphorene is 0.01. On the other hand, the Poissons ratio is generally believed to be rare in crystalline solids with only a few exceptional cases such as $\alpha-$ SiO_2[34] and cubic metals[35]. However, the negative Poisson seems to be more common in two-dimensional materials. Recently, a lot of two-dimensional materials including B-graphane,[23] single-layer honeycomb-like structure of silica,[36] stoichiometric silicene oxides[37] and black phosphorus.[32] More attention should be paid to two dimensional materials to find more novel materials with negative Poisson ratio.

4 Conclusion

The geometry, electronic structure, carrier effective mass and elastic properties of halogenated silicene XSi (X=F,Cl,Br, and I) in various conformers have been investigated from first-principles systemically. Our results indicate that the

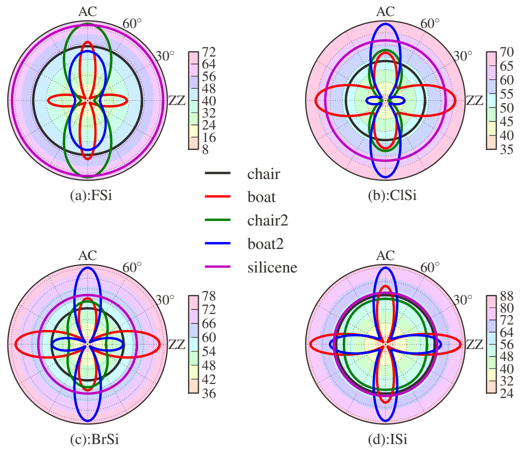

Fig. 6 (Color online) Polar diagram for the Young modulus E of halogenated silicene.(a)-(d) represent the FSi, ClSi , BrSi and ISi system, respectively. The angle θ identifies the extension direction with respect to the zigzag one. ZZ and AC represent the zigzag and armchair direction, respectively. The numerical values are represented by different background colors. Isotropic (anisotropic) behavior is associated to a circular (noncircular) shape of the E_n plot.

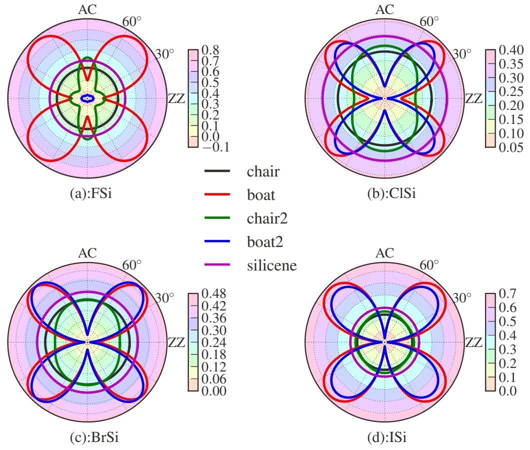

Fig. 7 (Color online) Polar diagram for the Poisson ratio ν of halogenated silicene.(a)-(d) represent the FSi, ClSi , BrSi and ISi system, respectively. The angle θ identifies the extension direction with respect to the zigzag one. ZZ and AC represent the zigzag and armchair direction, respectively. The numerical values are represented by different background colors. Isotropic (anisotropic) behavior is associated to a circular (noncircular) shape of the ν_n plot.

binding energy of halogenated silicene shows a strong element-dependence but is insensitive to conformer. The energy gaps of XSi given by semi-local PBE functional range from 0.54 to 2.08 eV and carrier effective masses are found to be small, which are comparable with conventional electronic materials. Moreover, elastic constants and direction-dependent mechanical properties of halogenated silicene are also calculated , and a negative Poisson ratio is predicted in fluorinated silicene with boat2 structure. The present results suggest halogenated silicene as the potential candidate in future electronic device.

5 Acknowledgement

This work was supported by the construct program of the key discipline in hunan province and aid program for Science and Technology Innovative Research Team in Higher Educational Institutions of Hunan Province.

References

1 S. Cahangirov, M. Topsakal, E. Aktürk, H. Şahin and S. Ciraci, *Phys. Rev. Lett.*, 2009, **102**, 236804.
2 D. Jose and A. Datta, *Accounts of Chemical Research*, 2014, **47**, 593–602.
3 B. Feng, Z. Ding, S. Meng, Y. Yao, X. He, P. Cheng, L. Chen and K. Wu, *Nano Letters*, 2012, **12**, 3507–3511.
4 P. Vogt, P. De Padova, C. Quaresima, J. Avila, E. Frantzeskakis, M. C. Asensio, A. Resta, B. Ealet and G. Le Lay, *Phys. Rev. Lett.*, 2012, **108**, 155501.
5 M. X. Chen and M. Weinert, *Nano Letters*, 2014, **14**, 5189–5193.
6 W.-F. Tsai, C.-Y. Huang, T.-R. Chang, H. Lin, H.-T. Jeng and A. Bansil, *Nat Commun*, 2013, **4**, 1500.
7 C.-C. Liu, W. Feng and Y. Yao, *Phys. Rev. Lett.*, 2011, **107**, 076802.
8 C.-C. Liu, H. Jiang and Y. Yao, *Phys. Rev. B*, 2011, **84**, 195430.
9 K. Nakada, M. Fujita, G. Dresselhaus and M. S. Dresselhaus, *Phys. Rev. B*, 1996, **54**, 17954–17961.
10 G. Gui, J. Li and J. Zhong, *Phys. Rev. B*, 2008, **78**, 075435.
11 F. Karlick, K. Kumara Ramanatha Datta, M. Otyepka and R. Zboil, *ACS Nano*, 2013, **7**, 6434–6464.
12 Q. Tang, Z. Zhou and Z. Chen, *Nanoscale*, 2013, **5**, 4541–4583.
13 E. Bianco, S. Butler, S. Jiang, O. D. Restrepo, W. Windl and J. E. Goldberger, *ACS Nano*, 2013, **7**, 4414–4421.
14 L. C. Lew Yan Voon, E. Sandberg, R. S. Aga and A. A. Farajian, *Applied Physics Letters*, 2010, **97**, 163114.
15 M. Houssa, E. Scalise, K. Sankaran, G. Pourtois, V. V. Afanasev and A. Stesmans, *Applied Physics Letters*, 2011, **98**, 223107.
16 J. C. Garcia, D. B. de Lima, L. V. C. Assali and J. F. Justo, *The Journal of Physical Chemistry C*, 2011, **115**, 13242–13246.
17 N. Gao, W. T. Zheng and Q. Jiang, *Phys. Chem. Chem. Phys.*, 2012, **14**, 257–261.
18 X. D. Wen, L. Hand, V. Labet, T. Yang, R. Hoffmann, N. W. Ashcroft, A. R. Oganov and A. O. Lyakhov, *Proceedings of the National Academy of Sciences*, 2011, **108**, 6833–6837.
19 Y. Ding and Y. Wang, *Applied Physics Letters*, 2012, **100**, 083102.
20 P. Giannozzi, S. Baroni, N. Bonini, M. Calandra, R. Car, C. Cavazzoni, D. Ceresoli, G. L. Chiarotti, M. Cococcioni, I. Dabo, A. D. Corso, S. de Gironcoli, S. Fabris, G. Fratesi, R. Gebauer, U. Gerstmann,

C. Gougoussis, A. Kokalj, M. Lazzeri, L. Martin-Samos, N. Marzari, F. Mauri, R. Mazzarello, S. Paolini, A. Pasquarello, L. Paulatto, C. Sbraccia, S. Scandolo, G. Sclauzero, A. P. Seitsonen, A. Smogunov, P. Umari and R. M. Wentzcovitch, *Journal of Physics: Condensed Matter*, 2009, **21**, 395502.

21 J. P. Perdew, K. Burke and M. Ernzerhof, *Phys. Rev. Lett.*, 1996, **77**, 3865–3868.

22 H. J. Monkhorst and J. D. Pack, *Phys. Rev. B*, 1976, **13**, 5188.

23 E. Cadelano, P. L. Palla, S. Giordano and L. Colombo, *Phys. Rev. B*, 2010, **82**, 235414.

24 S. Baroni, S. de Gironcoli, A. Dal Corso and P. Giannozzi, *Rev. Mod. Phys.*, 2001, **73**, 515–562.

25 A. Acun, B. Poelsema, H. J. W. Zandvliet and R. van Gastel, *Applied Physics Letters*, 2013, **103**, 263119.

26 P. D. Padova, C. Ottaviani, C. Quaresima, B. Olivieri, P. Imperatori, E. Salomon, T. Angot, L. Quagliano, C. Romano, A. Vona, M. Muniz-Miranda, A. Generosi, B. Paci and G. L. Lay, *2D Materials*, 2014, **1**, 021003.

27 F. Karlický, R. Zbořil and M. Otyepka, *The Journal of Chemical Physics*, 2012, **137**, 034709.

28 O. Leenaerts, H. Peelaers, A. D. Hernández-Nieves, B. Partoens and F. M. Peeters, *Phys. Rev. B*, 2010, **82**, 195436.

29 C. Q. Sun, *Progress in Solid State Chemistry*, 2007, **35**, 1 – 159.

30 M. Topsakal and S. Ciraci, *Phys. Rev. B*, 2010, **81**, 024107.

31 Q. Peng, X. Wen and S. De, *RSC Adv.*, 2013, **3**, 13772–13781.

32 J. W. Jiang and H. S. Park, *Nat Commun*, 2014, **5**, 4727.

33 Y. Ding, Y. Wang, L. Shi, Z. Xu and J. Ni, *physica status solidi (RRL) Rapid Research Letters*, 2014, **8**, 939–942.

34 N. R. Keskar and J. R. Chelikowsky, *Nature*, 1992, **358**, 222–224.

35 R. H. Baughman, J. M. Shacklette, A. A. Zakhidov and S. Stafstrom, *Nature*, 1998, **392**, 362–365.

36 V. O. Özçelik, S. Cahangirov and S. Ciraci, *Phys. Rev. Lett.*, 2014, **112**, 246803.

37 Y. Wang and Y. Ding, *physica status solidi (RRL) Rapid Research Letters*, 2013, **7**, 410–413.

Halogenated silicene, with an enhanced stability compared with silicene, present the moderate and tunable direct gap with small carrier effective mass, and improved Elastic properties.

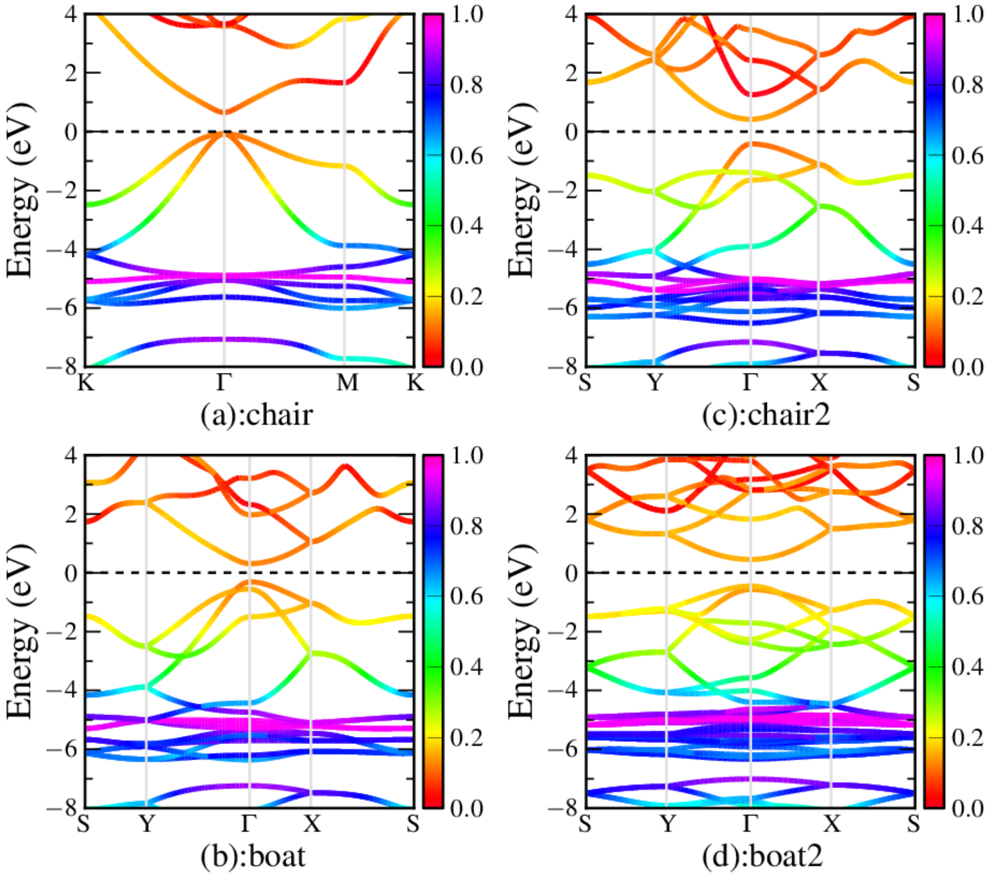

(a):chair

(c):chair2

(b):boat

(d):boat2